Published in final edited form as:
J Biomed Mater Res A. 2012 December ; 100(12): 3455–3462. doi:10.1002/jbm.a.34285.

Histocompatibility and *in vivo* Signal Throughput for PEDOT, PEDOP, P3MT and Polycarbazole Electrodes

Patrick. A. Forcelli[1,*], **Cameron T. Sweeney**[2,*], **Anthony D. Kammerich**[2], **Brian C-W. Lee**[2], **Laura H. Rubinson**[1,2], **Yohani P. Kayinamura**[2], **Karen N. Gale**[1], and **Judith F. Rubinson**[1,2]

[1]Department of Pharmacology and Physiology, Georgetown University, Washington, DC 20057

[2]Department of Chemistry, Georgetown University, Washington, DC 20057

Abstract

Stimulation and recording of the *in vivo* electrical activity of neurons are critical functions in contemporary biomedical research and in treatment of patients with neurological disorders. The electrodes presently in use tend to exhibit short effective lifespans due to degradation of signal transmission resulting from the tissue response at the electrode-brain interface, and the signal throughput suffers most at the low frequencies relevant for biosignals. To overcome these limitations, new electrode designs to minimize tissue responses, including conducting polymers have been explored. Here we report the short-term histocompatibility and signal throughput results comparing platinum and conducting polymer modified platinum electrodes in a Sprague-Dawley rat model. Two of the polymers tested elicited significantly decreased astrocyte responses relative to platinum. These polymers also showed improved signal throughput at low frequencies and comparable signal to noise ratios during targeted intracranial electroencephalograms (EEG). These results suggest that conducting polymer electrodes may present viable alternatives to the metal electrodes that are currently in use.

INTRODUCTION

Implanted electrodes have become a critical tool in research, diagnosis, and, more recently, treatment for neurological disorders [1–7] In designing improved electrodes for sensing and stimulation, a major challenge is that communication across a tissue-electrode interface. Optimal electrodes must overcome two major obstacles in the form of long-term tissue compatibility and fast response to signals [8], The first challenge has its origin in tissue response to a foreign body. This response results in glial scarring, which, in effect, forms an insulating interface that impedes signal transduction or charge injection for long-term implantation [6, 9–12]. In addition to the challenges posed by tissue reactivity, the interfacial impedance inherent in the sensing and stimulating electrodes currently available for medical use introduces a nonohmic time-dependent high-pass filter element at the low frequencies relevant for neural sensing or stimulation [12–17], (Typical biosignal frequencies are shown in Figure 1.)

This impedance is a particular problem in the case of sensing applications, where significant interfacial impedance (particularly the frequency-dependent capacitive component) results in a decrease in signal amplitude and lower signal-to-noise. The dual-threat combination of glial scarring and frequency-dependent response leads to outcomes in which low amplitude and/or low frequency contributions may well be filtered from the detected signal.

Corresponding Author: Judith F. Rubinson, Department of Pharmacology, SE402 Med-Dent, Georgetown University, 3900 Reservoir Rd, NW, Washington, DC 20057, Phone: 202-687-3627, jfr@georgetown.edu.
*These authors contributed equally to this work

In work stemming from cardiac electrode impedance measurements from [18], we reported in 2003 that it was possible to achieve low impedance, frequency-independent behavior over a limited range (25–806 Hz) for a subset of poly(3,4-ethylenedioxy-thiophene), or PEDOT, electrodes. Since that time, we have increased the useful frequency range for PEDOT [19] and have extended our investigations to other conducting polymer (CP) electrodes [20] for possible use in neural sensing applications.

Conducting polymers have shown a great deal of promise for use in conjunction with, and eventually as an alternative to, metal electrodes in clinical and laboratory conditions [21]. These polymers are comprised of repeating units of covalently-bonded monomers which, when oxidatively polymerized in the presence of anionic dopants, produce films with conductivities on the order of 100 $S\text{-}m^{-1}$ or greater [22]. The two conducting polymers on which we focus here are poly(3,4-ethylenedioxypyrrole) (PEDOP) and poly(3-methylthiophene) (P3MT) (Figure 2). PEDOT, the thiophene analog of PEDOP has been studied extensively and is currently the most widely investigated conducting polymer for coated-electrode studies [23–26]. The excellent results obtained with neuronal growth on polypyrrole fibers [27] under small applied potentials, combined with the fact that the ethylenedioxy substituent in PEDOT and PEDOP increases the electron density [28], and subsequently the conductivity, of the π-system through electronic induction from nonbonding oxygen electrons, suggested that it would be valuable to probe the effect of the heteroatom on its properties. Based on reports by Refaey [29], P3MT displays the same low impedance at low frequencies as PEDOT and PEDOP,[19] however, despite its high conductivity, P3MT has not been previously investigated for in vivo utility. Thus, in the present study we investigated the efficacy of conducting polymers (P3MT and PEDOP) for in vivo sensing and histocompatibility. We tested the hypothesis that these conducting polymers would display low impedance, frequency-independent behavior, while minimizing tissue damage.

To investigate signal throughput, we employed intracranial EEG recordings of seizure activity. An epilepsy model was chosen for testing of signal throughput. This model was selected because it is a common research (and clinical) application for *in vivo* electrodes. In these applications, both baseline and ictal (seizure) activity are monitored [2, 5]. Furthermore, the signals of interest contain low frequency elements, enabling us to test the hypothesis that these PEDOP and P3MT electrodes will provide improved signal throughput.

To investigate histocompatibility, we employed immunohistochemistry directed against astrocytic and microglial responses. Lesions, traumatic brain injuries, and other traumas (e.g. electrode implantations) lead to activation (proliferation, increase in organelle number, and increase in transcription) and migration of astrocytes to the injury site during, which approaches it maximum by 40–60 days post-injury. This astrocyte migration results in the glial scarring that is characteristic of the electrode-brain interface [30] The expression of glial fibrillary acidic protein (GFAP), an important intermediate filament that is specific to astrocytes, increases upon astrocyte activation and migration, making GFAP an effective marker for assessing gliosis post-trauma. Microglia represent the second component of the brain response to trauma. These cells are the resident macrophages of the central nervous system, and account for approximately 10% of the cells in the brain [5]. Microglia migrate to regions where foreign material has been introduced to phagocytize dying cells, while releasing proteolytic enzymes (i.e. hydrolase) to degrade damaged tissue [12, 31]. They also can be involved in the release of toxins such as superoxide and nitric oxide during inflammatory response [32–34]. Upon activation, microglia express the cell surface marker, CD11b. Thus, we have chosen CD11b as a marker of microglial response [35, 36].

Through a combination of histopathological and *in vivo* signal throughput analyses, the studies reported here suggest that the careful selection of conducting polymer can provide for low impedance, frequency-independent behavior while minimizing tissue damage.

MATERIALS AND METHODS

Fabrication of electrodes for tissue response assessment

Platinum electrodes were fabricated from 0.250 mm wire (99.998%, Alfa Aesar) as previously described [37]. Deposition was carried out using a standard three electrode cell configuration controlled by a Radiometer 80 or Radiometer 10 potentiostat (Hach) and Voltamaster 4 software. The auxiliary electrode was 0.500 mm diameter platinum wire (99.9998%, Alfa Aesar). A double junction Ag/AgCl reference electrode was used to interface the aqueous reference electrode to the electrodeposition cell. Polymer was deposited using a cyclic voltammetric protocol on each working electrode, replacing the deposition solution after every five electrodes. Electrodes were visually inspected using an optical microscope before use to insure that the surface was completely covered and were tested before use by cyclic voltammetry (CV) between −0.1 and +0.6 V vs Ag/AgCl to check for excessive background current (i >100 μA/cm^2 at extremes of scan).).

Fabrication of electrodes for signal throughput assessment

Two-channel twisted wire electrodes (Plastics1 MS303/6-B/SPC), with platinum wires that extended 4 mm below the pedestal and were insulated with Teflon except at the tip, were employed. The exposed platinum surface was coated using the same standard three-electrode setup previously discussed, with deposition solution conditions and deposition times adjusted to completely coat the exposed surface of each electrode but prevent overlap of the coating between the electrodes. Each channel (in succession) was connected to the potentiostat as the working electrode. Each electrode was examined under a microscope after coating and a sharp blade was run between the 2 channels to remove any fibers not visible.

Electrode Implantation

A total of 40 adult male Sprague-Dawley rats (~300g) underwent surgical implantation of electrodes for these studies. Rats were anesthetized with equithesin (a combination of sodium pentobarbital, chloral hydrate, magnesium sulfate, ethanol, and propylene glycol) (2.5ml/kg, i.p.) prior to stereotaxic placement of electrodes.

In each animal, platinum electrode(s) were placed unilaterally, with coated electrodes placed contralaterally. This approach allowed each animal to serve as its own control. While there are several reports of contralateral gliosis/neuroinflammation following unilateral stab trauma [38–40], the pattern of gliosis is typically diffuse and mild, markedly different than the pattern at the injury site.. Furthermore, several other reports have shown a lack of tissue response at sites contralateral to implanted electrodes [9, 11]. The number of animals per group, and the type and position of electrodes for both histocompatibility and signal throughput experiments are summarized in Table 1.

For histocompability studies, electrodes were implanted bilaterally in hippocampus (coordinates relative to bregma: AP:−4.16mm, ML:±2.5mm, DV: −4mm) and striatum (coordinates to bregma: AP: +0.7mm, ML: ±2.5mm, DV: −6mm) and affixed to the skull with four jeweler’s screws and dental acrylic, as we have previously described [41].

For signal throughput studies, 20 animals were used. For each animal, electrodes were implanted bilaterally in the hippocampus, with a polymer electrode in one hemisphere and a platinum electrode in the contralateral hemisphere, as previously described[41].

Post-operative analgesia (e.g., a non-steroidal anti-inflammatory drug) was not provided in order to avoid interference with tissue responses. All animals recovered without difficulty, and were monitored for adverse affects for the duration of the study. All animal procedures and euthanasia were carried out using protocols approved by the Georgetown University Animal Care and Use Committee (GUACUC).

Immunohistochemistry

Fourteen days post-surgery, animals were euthanized and perfused with phosphate buffered saline, followed by 4% paraformaldehyde. Electrodes were carefully retracted from the brain after perfusion. Brains were removed and postfixed for 24 hours in paraformaldehyde, cryoprotected through graded sucrose solutions, and frozen on dry ice prior to cryosectioning. Horizontal sections (perpendicular to the electrode track, with a thickness of 20 μm) were slide-mounted and stored at −80C until histochemical processing. Adjacent tissue sections were stained using an immunofluorescent protocol to detect GFAP or CD11b, allowing us to access the tissue response at the electrode implantation site.

GFAP—Slides were incubated in 100% methanol for 15 minutes at −20°C, and then washed for 3 minutes in phosphate buffer. Antigen retrieval was performed by pulse heating the slides in citrate buffer (25 seconds heat, 1 minute cool) so that the temperature stayed ~95°C for 20 minutes. Slides were washed 2 times in PBS for three minutes, and then blocked (1% bovine serum albumin, 0.3%Triton-X-100, 20% goat serum in PBS) for 1 hour. Slides were then incubated with the primary antibody (1:500, rabbit α GFAP, ab7779-800, Abcam) overnight at room temperature. Slides were washed, and then incubated with secondary antibody (1:500, Alexa Fluor 546 from Invitrogen FITC goat α rabbit) for 1h at room temperature. Slides were washed then coverslipped with Cytoseal-60.

CD11b—Slides were blocked (5% normal goat serum, 1% bovine serum albumin, 0.3%Triton-X 100 in PBS) for one hour at room temperature. The slides were incubated with the primary antibody (1:200, mouse α CD11b, ab8878 from Abcam) overnight at room temperature, and then incubated with the secondary antibody (1:250, goat α mouse, AlexaFluor 488, Invitrogen) for one hour at room temperature. Slides were then washed and then coverslipped with Cytoseal-60.

Fluorescence Quantitation

Images were obtained using a Nikon E600 Fluorescent Microscope and Nuance v2.4 Multispectral Imaging software (Cambridge Research & Instrumentation, Inc. (CRi)). Quantification of immunofluorescence was performed using ImageJ. Image collection and analysis was performed by a treatment-blind observer (C.T.S).

A band, extending approximately 225 μm from the center of the electrode track was outlined by hand, with the electrode track excluded. The remaining area comprises (a toroidal band which extends approximately 100 μm outside the edge of the electrode track. We selected this area based on preliminary investigations showing the highest level of tissue response in this peri-electrode region. The fluorescence intensity of the toroidal band was then quantified, representing the brain-electrode interface. The total area of the band was measured and fluorescence was normalized to the area analyzed. This procedure was repeated for at least four sections per electrode track, spaced at 200um.

EEG sensing

Two or fourteen days after electrode implantation, rats were subjected to electrographic recordings (Grass Model 8-Plus; data acquired using PolyView16, bandpass 1 Hz, 60 Hz, 1280 points/s). Simultaneous (platinum vs. modified platinum) baseline data was obtained and recorded for a minimum of 10 minutes to ensure that a stable background signal was obtained. Following the baseline recordings, animals were injected with pentylenetetrazole (PTZ, 30–40mg/kg, i.p.) to evoke ictal electrographic responses. Simultaneous data indicative of seizure activity was obtained for at least five minutes. After these experiments, the animals were euthanized using an accepted protocol.

RESULTS AND DISCUSSION

A preliminary qualitative screening compared astrocyte response on implantation of platinum with that for PEDOP, PEDOT, polycarbazole (PCz) and P3MT electrodes. For P3MT, a trial was also carried out for a “fuzzy” electrode to assess whether small fibers might induce a greater response close to the electrode, either inherently or through fracture on insertion or movement. These preliminary assessments suggested that PEDOP elicited the lowest astrocyte response. (Typical images are included as Supplement 1). The next smallest astrocyte response occurred in the case of P3MT (both fuzzy and smooth). The difference in texture of the P3MT electrodes did not appear to alter the total astrocyte response, although fuzzy P3MT seemed to evoke a slightly greater response directly at the electrode-brain interface. The other three electrode types varied in response PCz < platinum < PEDOT.

It is worth noting that although we found PEDOT evoked a greater astrocyte response than platinum electrodes, this result must be evaluated in the context of the conditions employed for deposition in this study. The electrodes evaluated by Cui and Martin [24] were produced under very different conditions (aqueous solution in which polystyrene sulfonate acts as both surfactant and counterion dopant)[23, 24, 26]. The use of polyelectrolytes as counterions has been shown to produce more mechanically stable polymer fibers and thus may well result in less damage on insertion. This advantage was balanced against our goal of increased signal throughput at low frequencies, a property associated with smaller counterions [20, 42].

Based on the results of our preliminary assessments, we performed a detailed quantitative comparison of P3MT and PEDOP with bare platinum electrodes. Astrocytic response was clearly present under all electrode conditions (Figure 3a). Quantification of immunofluorescence at the brain-electrode interface revealed a significantly attenuated response in the polymer-coated electrodes as compared to the uncoated platinum electrode (Figure 3b; $F_{2,21}=5.795$, $p<0.01$, $p<0.05$ Dunnett’s multiple comparison test).

Microglial response: PEDOP and P3MT

Microgliosis (as indicated by CD11b expression) was present under all electrode conditions (Figure 4a). The activated microglial response, unlike that observed for astrocytosis, was not attenuated by the use of polymer-coated electrodes (Figure 4b, $F_{2,24}=0.34$ $p=0.72$). In an isolated case in which a small fragment of P3MT flaked from one of the electrodes, the response in the area surrounding the site also was assessed (Supplement 2). The microglial response was lower than the P3MT average (0.018 vs. 0.029), suggesting that the majority of the microglial response is due to the insertion trauma, but further evidence is required to substantiate this suggestion.

Signal throughput during EEG sensing

Power spectral analysis was carried out on 2-minute segments of the baseline and ictal periods of electrographic recording for each animal. Figure 5 shows the parallel responses of platinum and P3MT during a baseline and during a seizure segment. The close correspondence of the timing of the spikes in response during the seizure traces indicates that analogous regions have been targeted. These low-frequency, high amplitude spikes present are characteristic of seizure activity, and were accompanied by behavioral seizure manifestations in all animals.

Detection of a much larger amplitude response at the P3MT electrode was typical; this pattern was seen for five out of seven electrodes during the seizure traces. For the other two electrodes the signals were more comparable (within a factor of two of one another). and for all (seven out of seven) of the baselines traces. For PEDOP, the signal magnitudes were more comparable for all signals measured.

The traces also were analyzed to determine the power spectral density (PSD) across the frequency range accessed by our recording ($1 < f < 60$ Hz). The PSD is an indicator of the electrode response as a function of frequency, and comparison of the PSD results for platinum, PEDOP and P3MT provides evidence regarding the relative efficiency of signal throughput across the frequency range probed.

Spectra for each electrode under baseline and seizure conditions were normalized (the response at each point in the spectrum relative to that at the frequency of maximum response), and average spectra were generated for each electrode type under both baseline and seizure conditions, at both 2 and 14 day post-implant time points (Figure 6). Four 5-Hz frequency windows (i.e., 1–5Hz, 5–10Hz, 10–15Hz, and 15–20Hz) were analyzed by ANOVA with Dunnet's post-hoc test. Table 2 provides a summary of the ANOVA results for comparison of the normalized PSD curves for the two polymers with platinum.

Two days after electrode implantation, signal throughput was significantly greater for polymer electrodes, as compared to platinum electrodes. Under seizure conditions, the polymer response was equivalent at low frequencies, and attenuated at high frequencies. Fourteen days after electrode implantation, greater signal throughput was detected for PEDOP (1–5Hz) and P3MT (5–10Hz) under baseline conditions; as compared to platinum electrodes, signal throughput was significantly greater for P3MT (5–20Hz), and significantly lower for PEDOP (5–20 Hz) under seizure conditions. (It is important to note that "baseline" does not mean "no signal." it corresponds to normal hippocampal neural signals.)At both two and fourteen days after implantation, the two conducting polymers produced power spectra that were not statistically different from that of platinum at the lowest frequencies (< 5Hz).

A point worth considering is the degree to which tissue responses interacted with signal throughput. It is possible that the improved signal we detected with P3MT electrodes at 14 days post-implantation reflect the decreased astrocytic response, which may result in reduced interfacial impedance and improved signal throughput. However, the fact that we detected improved signal throughput for both polymer electrodes at two days after implantation, a time when the tissue response is still in the active phase, and glial scarring is far from complete, suggests that improved signal throughput is also a function of inherently lower impedance at these frequencies at the polymer coated electrodes. This is consistent with the solution studies carried out in our group [20].

CONCLUSIONS

Although this study was of limited duration, the results reported here show that both PEDOP-coated and P3MT-coated electrodes produce lower levels of astrocyte activation in the area immediately surrounding the electrode track compared to platinum. The immunofluorescent analysis of the brain-electrode interface may offer increased sensitivity as compared to an immunohistochemical approach and allowed for the normalization of fluorescent signal to the region of tissue surrounding the electrode track. It is important in evaluating the astrocyte results presented above to note that this study observed the tissue responses only two weeks post-implantation. The astrocytic gliosis surrounding neuronal trauma is not usually complete and stable until after about six weeks [12]. Although gliosis is considered somewhat diffuse at the second week post-implantation, our results show that the glial scar had begun to become more compact by week two. The microglial, response is generally complete by the second week post-implantation, and such a microglial sheath present at week two has been found to be present until at least week twelve post-implantation [12]. The extent of microglial activation and migration to the surrounding band at week two is a direct representation of the tissue response expected on a longer time scale. Although not statistically significant, PEDOP-coated and P3MT-coated electrodes appear to elicit smaller microglial responses relative to platinum electrodes in this same area. While microglial response is sustained after injury, peak responses after lesions have been reported within 2 d post-injury. Future investigations of tissue response as a function of time (with both shorter and longer survival times) would be of particular interest in resolving this issue.

Signal amplitude is generally greater for P3MT and PEDOP compared to platinum, and the power spectral density appears to be equivalent or, in several cases, superior for the polymers compared to bare platinum. This result is encouraging in view of prior results from our laboratory which indicate that deposition of a gold layer before polymer deposition leads to further improvement in low frequency signal throughput [19]. Investigation of these platinum/gold/conducting polymer (Pt/Au/CP) electrodes is the subject of ongoing studies in our laboratory. Polycarbazole (PCz) is also under investigation in our laboratory as it provides the same heteroatom as PEDOP, but with a more rigid, polyaromatic backbone. Although at frequencies <100 Hz the impedance is higher than that of PEDOT, PEDOP, and P3MT, the impedance is still significantly less than that of noble metal or PEDOP/PSS electrodes. [19]

Supplementary Material

Refer to Web version on PubMed Central for supplementary material.

Acknowledgments

The authors wish to acknowledge support from the Department of Chemistry and the Center for the Brain Basis of Cognition of Georgetown University. Partial support for acquisition of the FESEM instrument employed was provided by NSF DMR-521170. PAF was supported by a Predoctoral Fellowship from the Epilepsy Foundation, F31NS066822, and by NIH training grants T32DA007291 and T32NS041231.

References

1. Sunderam S, Bluckman B, Reato D, Bikson M. Toward rational design of electrical stimulation strategies for epilepsy control. Epileps Behav. 2010; 17:6–22.
2. Sunderam, S.; Chernyy, N.; Mason, J.; Peixoto, N.; Weinstein, SL.; Schiff, SJ., et al. Seizure Modulation with Applied Electric Fields in Chronically Implanted Animals. 28th IEEE EMBS Annual Internation Conference; 2006; 2006. p. 1612-1615.

3. Sunderam S, Talathi SS, Lyubushin A, Sornette D, Osorio I. Challenges for emerging neurostimulation-based therapies for real-time seizure control. Epileps Behav. 2011; 22:118–125.
4. Osorio I, Frei MG, Sunderam S, Giftakis J, Bhavaraju NC, Schaffner SF, et al. Automated Seizure Abatement in Humans Using Electrical Stimulation. Ann Neurol. 2005; 57:258–268. [PubMed: 15668970]
5. Richardson KA, Gluckman BJ, Weinstein SL, Glosch CE, Moom JB, Gwinn RP, et al. In Vivo Modulation of Hippocampal Epileptiform Activity with Radial Electric Fields. Epilepsia. 2003; 44:768–777. [PubMed: 12790889]
6. Butson CR, Miller IO, Normann RA, Clark GA. Selective neural activation in a histologically drived model of peripheral nerve. J Neural Eng. 2011; 8:036009. (036009 pp). [PubMed: 21478574]
7. Kipke DR. Silicon-Substrate Intracortical microelectrode Arrays for Long-Term Recording of Neuronal Spike Activity in Cerebral Cortex. IEEE Trans Neural Systems Rehab Eng. 2003; 11:151–155.
8. Cogan S. Neural Stimulation and Recording Electrodes. Annu Rev Biomed Eng. 2008; 10:275–309. [PubMed: 18429704]
9. Griffith RW, Humphrey DR. Long-term gliosis around chronically implanted platinum electrodes in the Rhesus macaque motor cortex. Neurosci Lett. 2006; 406:81–86. [PubMed: 16905255]
10. Kim Y-T, Hitchcock RW, Bridge MJ, Tresco PA. Chronic response of adult rat brain tissue to implants anchored to the skull. Biomaterials. 2004; 25:2229–2237. [PubMed: 14741588]
11. Freire MAM, Morya E, Faber J, Santos JR, Guimaraes JS, Lemos NAM, et al. Comprehensive Analysis of Tissue Preservation and Recording Quality from Chronic Multielectrode Implants. PLoS One. 2011; 6:e27554. 27510.21371/journal.pone.0027554. [PubMed: 22096594]
12. Polikov VS, Tresco PA, Reichart WM. Response fo brain tissue to chronically implanted neural electrodes. J Neuro Meth. 2005; 148:1–18.
13. Chou HA, Frenkel D, Ovadia M. Determination of standard electrode potential E° for chronic platinum and gold electrodes in rat muscle: Implications for biosensors and the “anode” of bipolar pacing. PACE. 2002; 25:1053–1060. [PubMed: 12164446]
14. Chou HA, Ovadia M, Moskowitz M, Zavitz DH. In Vivo Potentiostatic Studies at the Electrode-Tissue Interface: Filter properties of the monophasic Action Potential (Ag/AgCl) Electrode in Living Rat Heart. PACE. 2000; 23:386–394. [PubMed: 10750142]
15. Ovadia M, Zavitz DH. The electrode-tissue interface in living heart: equivalent circuit as a function of surface area. Electroanal. 1998; 10:262–272.
16. Ovadia M, Zavitz DH. Impedance spectroscopy of the electrode-tissue interface in living heart with isoosmotic conductivity perturbation. Chem Phys Lett. 2004; 390:445–453.
17. Wei XF, Grill WM. Current density distributions, field distributions and impedance analysis of segmented deep brain stimulation electrodes. J Neural Eng. 2005; 2:139–147. [PubMed: 16317238]
18. Ovadia M, Zavitz DH, Rubinson JF, Park D, Chou HA. Investigation of a semiconductor bioelectrode with Ohmic behavior in vivo: Impedance spectroscopy of p-type semiconductor electrodes in perfused living heart. Chemical Physics Letters. 2006; 419(1–3):277–287.
19. Kayinamura YP, Ovadia M, Rubinson JF. Investigation of Near Ohmic Behavior for Poly(3,4-ethylenedioxythiophene): A Model Consistent with Systematic Variations in Polymerization Conditions. ACS Appl Mater Interfaces. 2010; 2(9):2653–2662. [PubMed: 20715789]
20. Kayinamura, Y.; Roberts, J.; Rubinson, J. ACS Appl Mater Interfaces. 2012. Near-Ohmic Behavior for Conducting Polymers: Extension Beyond PEDOT on Gold-Plated Platinum to Other Polymer-Counterion/Substrate Combinations. published on web 2/2/2012
21. Ovadia M, Zavitz DH, Rubinson JF, Park D-G, Chou HA. Investigation of a semiconductor bioelectrode with Ohmic behavior in vivo: Impedance spectroscopy of p-type semiconductor electrodes in perfused living heart. Chem Phys Lett. 2006; 419(1–3):277–287.
22. Heeger A. Semiconducting and Metallic Polymers: The Fourth Generation of Polymeric Materials. J Phys Chem B. 2001; 105(36):8475–8491.
23. Cui X, Martin DC. Fuzzy gold electrodes for lowering impedance and improving polymer adhesion with electrodeposited conducting polymer films. Sensor Actuat A-Phys. 2003; 103(3): 384–394.

24. Cui X, Martin DC. Electrochemical deposition and characterization of poly(3,4-ethylenedioxythiophene) on neural microelectrode arrays. Sensor Actuat B-Chem. 2003; 89:92–102.
25. Ludwig KA, Uram JD, Yang J, Martin DC, Kipke DR. Chronic Neural recordings using silicon microelectrode arrays electrochemically deposited with a poly(3,4-ethylenedioxythiophene) (PEDOT) film. J Neural Eng. 2006; 3(1):59, 57. [PubMed: 16510943]
26. Xiao Y, Cui Z, Hancock JM, Bouguettaya M, Reynolds JR, Martin DC. Electrochemical polymerization of poly(hydroxymethylated-3,4-ethylenedioxythiophene) (PEDOT-MEOH) on multichannel neural probes. Sensor Actuat B-Chem. 2004; 99:437–443.
27. Schmidt CE, Shastri VR, Vacanti JP, Langer R. Stimulation of neurite outgrowth using an electrically conducting polymer. P Natl Acad Sci USA. 1997; 94:8948.
28. Thomas CA, Zong K, Schottland P, Reynolds JR. Poly(3,4-alkenedioxypyrrole)s as Highly Stable Aqueous-Compatible Conducting Polymers with Biomedical Implications. Adv Mater. 2000; 12:222.
29. Refaey SAM. Electrochemical impedance studies on the electrochemical properties of poly(3-methylthiophene) in aqueous solutions. Synthetic Met. 2004; 140:87–94.
30. Turner JN, Shain W, Szarowski DH, Andersen M, Martins S, Issacson M, et al. Cerebral astrocyte response to micromachined silicon implants. Exp Neurol. 1999; 156(1):33–49. [PubMed: 10192775]
31. Thomas WE. Brain macrophages: on the role of pericytes and perivascular cells. Brain Res Rev. 1999; 31:42–57. [PubMed: 10611494]
32. Guilian D, Baker TJ. Characterization of amoeboid microglia isolated from developing mammalian brain. J Neurosci. 1986; 6(8):2163–2174. [PubMed: 3018187]
33. Zielasek J, Mueller B, Hartung HP. Inhibition of cytokine-inducible nitic oxide synthase in rat microglia and mmurine macrophages by methyl-2,5-dihydroxycinnamate. Neurochem Int. 1996; 29(1):83–87. [PubMed: 8808792]
34. Shimoji M, Pagan F, Healton E, Mocchetti I. CXCR4 and CXCL12 Expresion is increased in the Nigro-Striatal Systems of Parkinson's Disease. Neurotox Res. 2009; 16:318–328. [PubMed: 19551455]
35. Sadhu, C. UCSD Nature Molecule Pages. 2007. Integrin alpha M.
36. Roy A, Jana A, Yatish K, Freidt MB, Fung YK, Martinson JA, et al. Reactive oxygen species up-regulate CD11B in microglia via nitric oxide: Implications for neurodegenerative diseaes. Free Radic Biol Med. 2008; 45:686–699. [PubMed: 18590811]
37. Kammerich AD, Srivastava Y, Hargett KN, Harrison VSR, Rubinson JF. Preparation of Microfiber and Smooth Film Conducting Polymer Electrodes. J Electrochem Soc. 2009; 156(4):P68–P73.
38. Jaquins-Gerstl A, Shu Z, Zhang J, Liu Y, Weber SG, Mchael AC. Effect of Dexamethasone on Gliosis, Ischemia, and Dopamine Extraction during Microdialysis Sampling in Brain Tissue. Anal Chem. 2011; 83:7662–7667. [PubMed: 21859125]
39. Moumdjian FA, HO, Abtek, Yong VW. Origin of contralateral reactive gliosis in surgically injured rat cerebral cortex. Brain Research. 1991; 547:223–228. [PubMed: 1884197]
40. Holguin A, Frank MG, Biedenkapp JC, Nelso K, Lippert D, Watkins LR, et al. Characterization of the temporo-spatial efffects of chronic bilateral intrahippocampal cannulae on interleukin-1β. J Neurosci Methods. 2007; 161:265–272. [PubMed: 17241670]
41. Forcelli PA, West EA, Murnen AT, Malkova L. Ventral Pallidum Mediates Amygdala-Evoked Deficits in Prepulse Inhibition. Behavioral Neuroscience. 2012; 126:290–300. [PubMed: 22250771]
42. Elschner, A.; Kirchmeyer, S.; Lovenich, W.; Merker, U.; Reuter, K. PEDOT: Principles and Applications of an Intrincially Conductive Polymer. Boca Raton, Fl: CRC Press (Taylor and Francis Group, LLC); 2011.

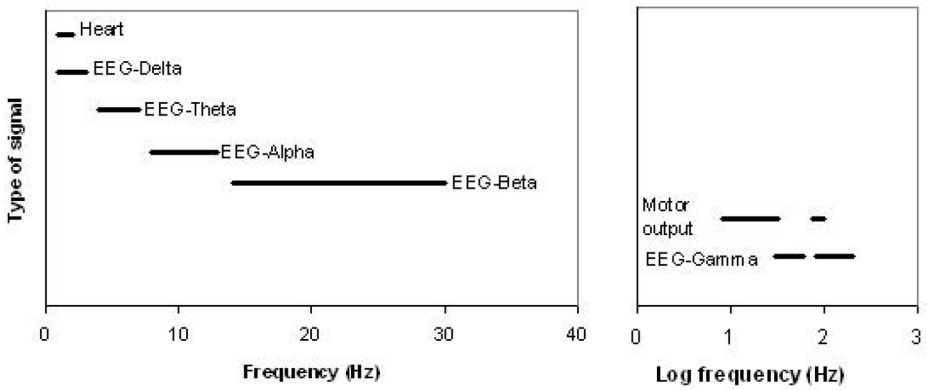

Figure 1.
Typical biosignal frequency ranges

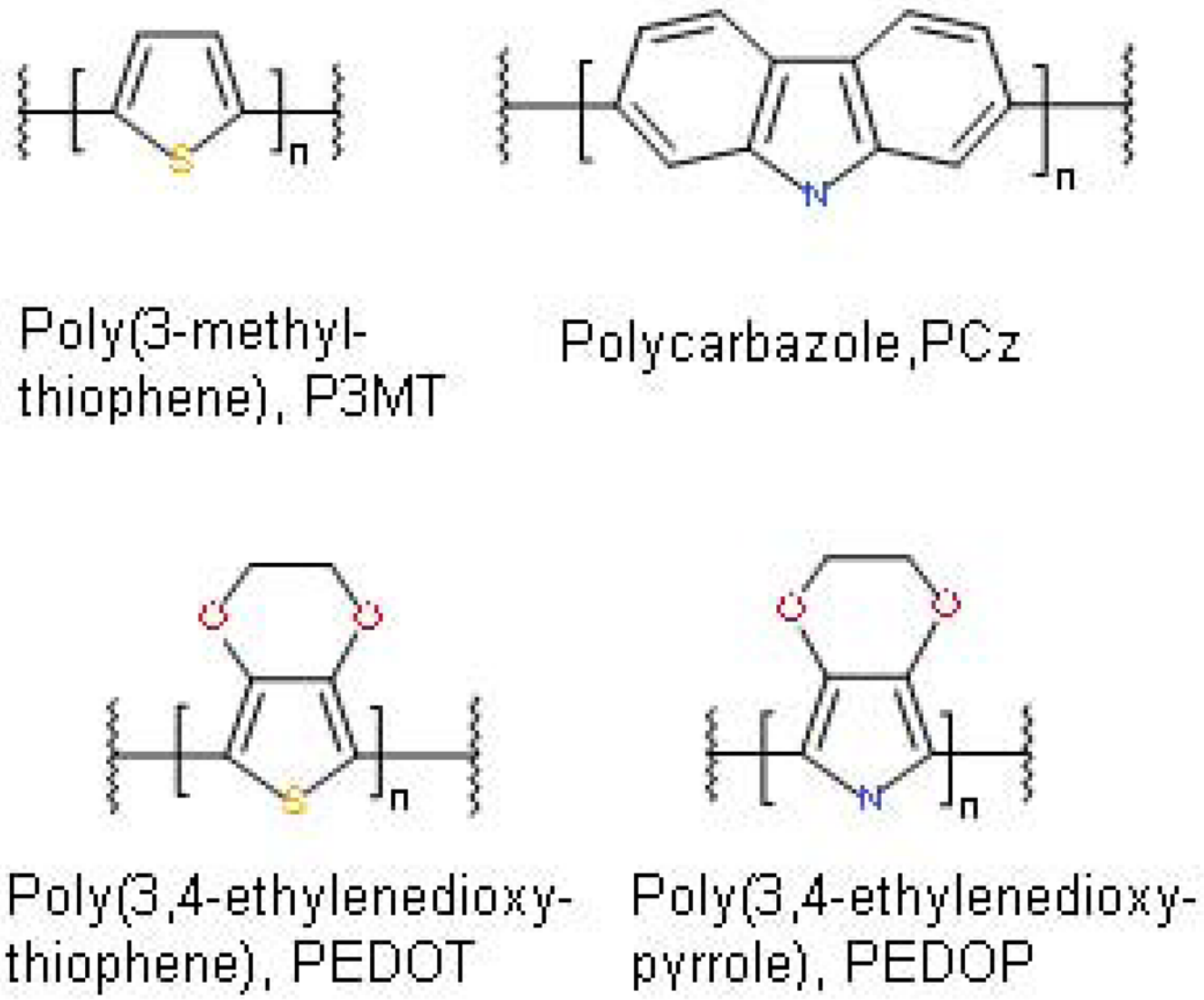

Figure 2.
Polymers investigated

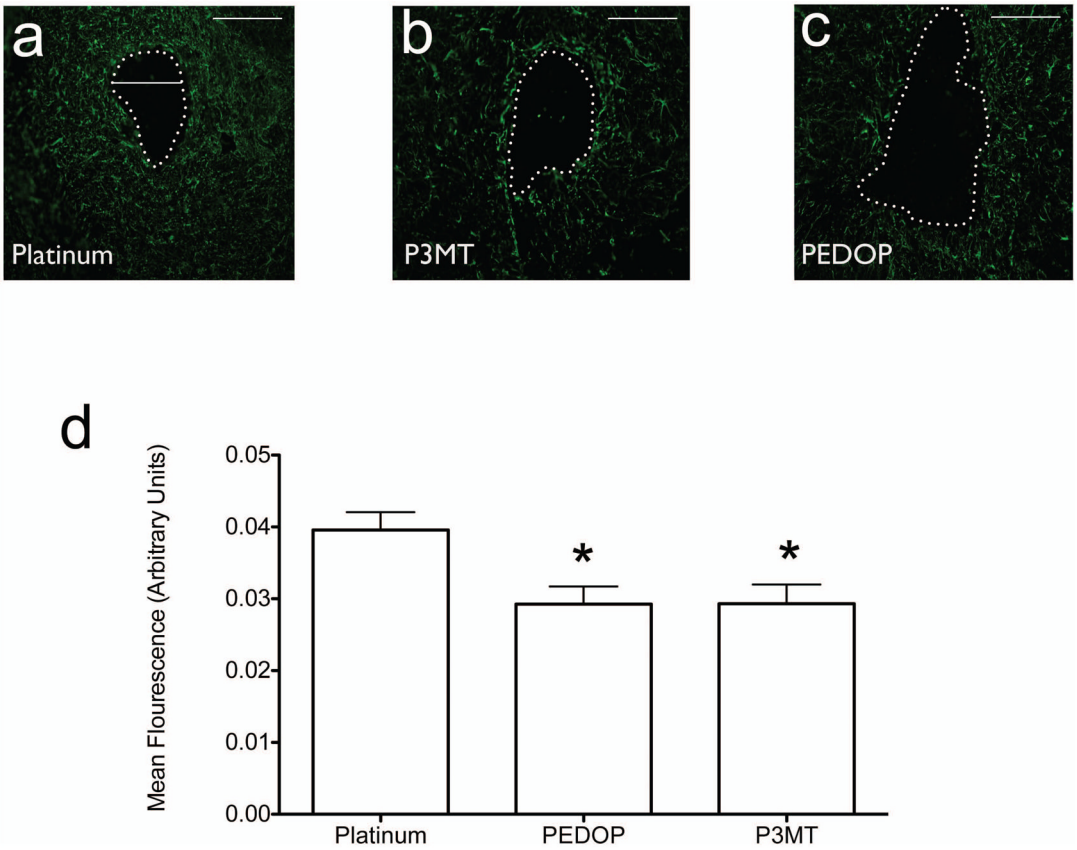

Figure 3.

Astrocyte response to implanted electrodes. (a–c) Typical responses, with electrode track denoted, to platinum, P3MT, and PEDOP, respectively. (d) Summary of responses for all animals tested. Number of animals tested: Platinum, n=11, P3MT, n=6, PEDOP, n=7. Standard errors are indicated for each type of electrode. *=significant difference for both Pt vs P3MT and for Pt vs PEDOT. *p* values are specified in the text. Scale marker in (a)–(c) corresponds to 250 microns.

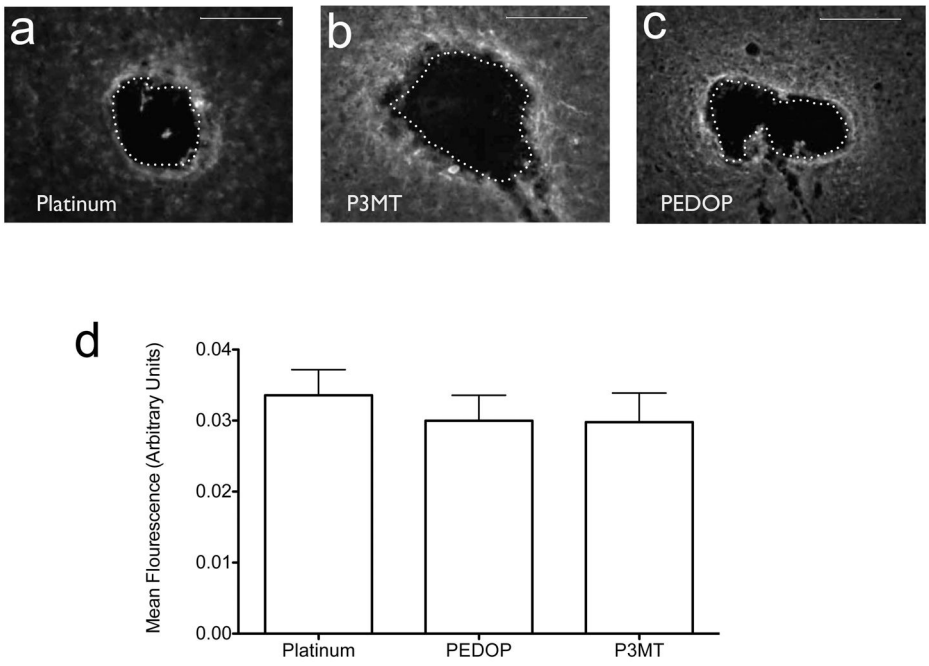

Figure 4.

Microglial response to implanted electrodes. (a–c) Typical responses, with electrode track denoted, to platinum, P3MT, and PEDOP, respectively. Magnification factor: (d) Summary of responses for all animals tested. Number of animals tested were: Platinum, n=10, P3MT, n=8, PEDOP, n=9. Standard errors are indicated for each type of electrode. Scale marker in (a)–(c) corresponds to 250 microns.

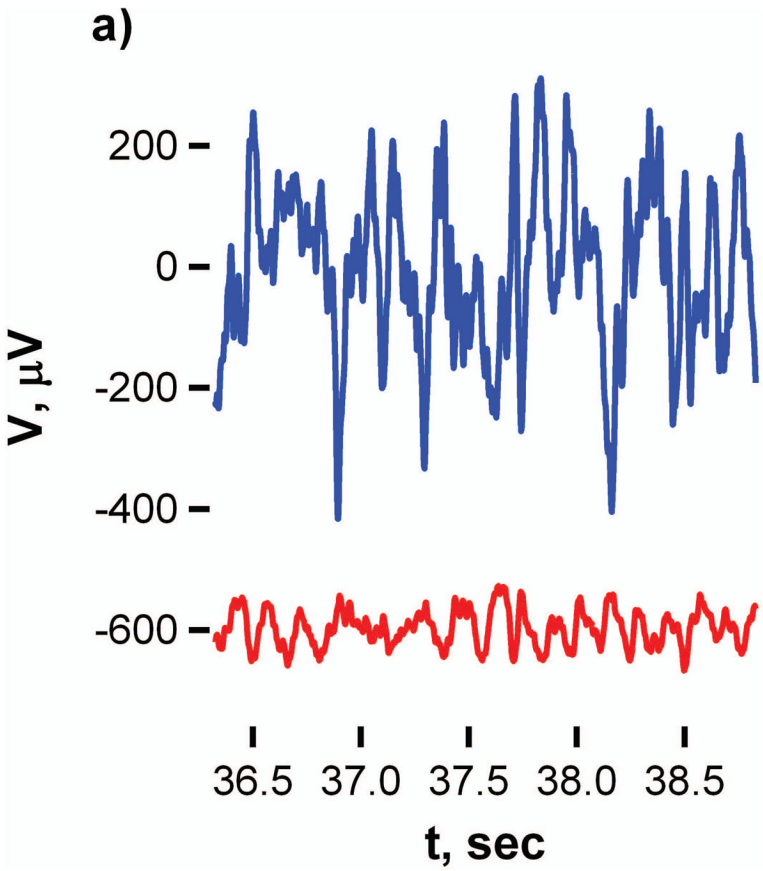

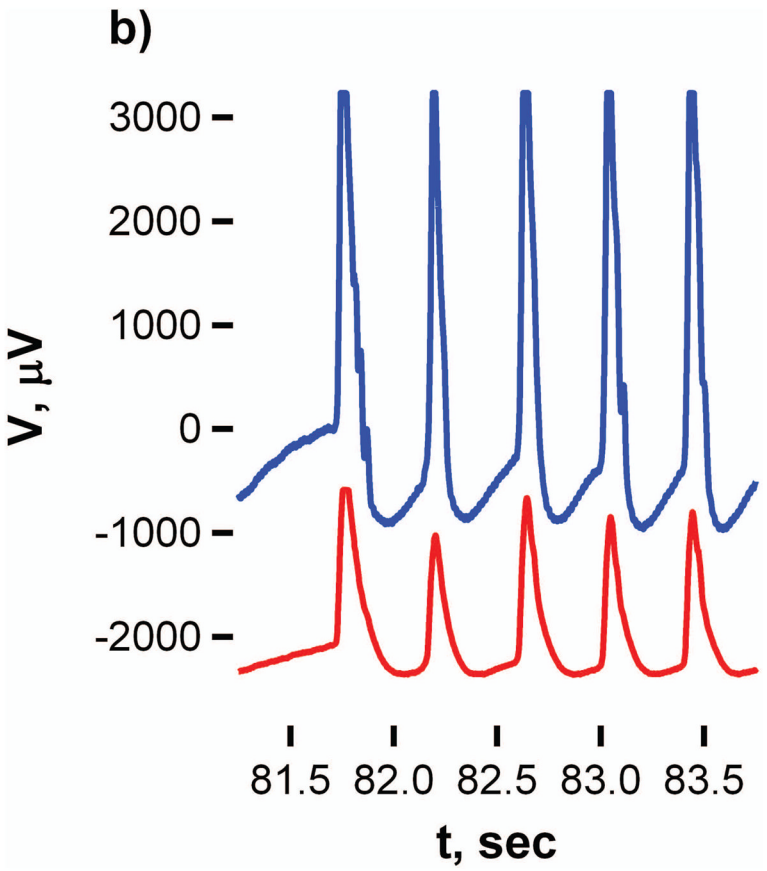

Figure 5.
Comparison of EEG signals for platinum (red line) and P3MT (black line) at 14 days post implant.

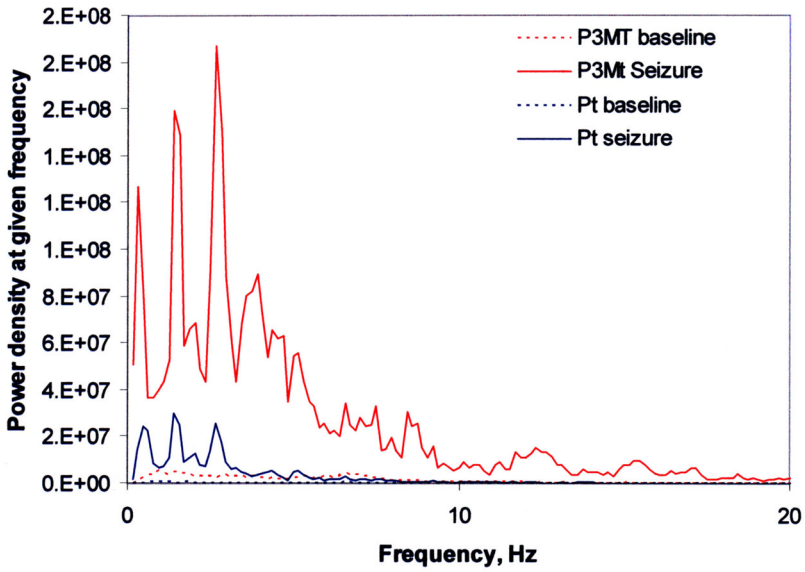

Figure 6.
Comparison of power spectral density at low frequency for P3MT and platinum at 14 days

Table 1

Summary of animal numbers for in vivo testing

Group	N=	Description of Electrodes/Implant Sites
Histocompatibility Pilot Studies (Supplement 1**)**	9	1 electrode placed per hemisphere
PEDOP	2	PEDOP electrodes placed unilaterally in the striatum and hippocampus; platinum electrodes in the contralateral striatum and hippocampus
PEDOT	2	PEDOT electrodes placed unilaterally in the striatum and hippocampus; platinum electrodes in the contralateral striatum and hippocampus
P3MT (smooth)	2	P3MT (smooth) electrodes placed unilaterally in the striatum and hippocampus; P3MT (fuzzy) electrodes in the contralateral striatum and hippocampus
P3MT (fuzzy)	1	P3MT (smooth) electrodes placed unilaterally in the striatum and hippocampus; P3MT (fuzzy) electrodes in the contralateral striatum and hippocampus
Polycarbazole (PCz)	2	PCz electrodes placed unilaterally in the striatum and hippocampus; P3MT (fuzzy) electrodes in the contralateral striatum and hippocampus
Histocompatibility (Figures 3 and 4)	11	1 electrode placed per hemisphere
P3MT (smooth)	5	PEDOP electrodes placed unilaterally in the striatum and hippocampus; platinum electrodes in the contralateral striatum and hippocampus
PEDOP	5	PEDOP electrodes placed unilaterally in the striatum and hippocampus; platinum electrodes in the contralateral striatum and hippocampus
PEDOP	1	PEDOP electrode placed unilaterally in the hippocampus; platinum electrode in the contralateral hippocampus
Signal Throughput (Figures 5 and 6)	20	Paired electrode placed in hippocampus of each hemisphere
P3MT (smooth)	9	P3MT placed unilateral, platinum contralaterally
PEDOP	11	PEDOP placed unilateral, platinum contralaterally

Table 2

Comparison of normalized power spectral density curves

Day	Period	Polymer	0<f≤5	$F_{2,62}$	5<f≤10	$F_{2,62}$	10<f≤15	$F_{2,62}$	15<f≤20	$F_{2,62}$
2	Baseline	P3MT	****	22.97	****	64.94	****	144.5	*	156.6
		PEDOP	****		****		****		****	
	Seizure	P3MT	ns	0.1661	****	139.4	****	241.1	****	301
		PEDOP	ns		****		****		****	
14	Baseline	P3MT	ns	3.649	*	33.56	ns	18.58	ns	1.162
		PEDOP	**		****		****		ns	
	Seizure	P3MT	ns	1.63	****	61.63	**	206.9	****	144.1
		PEDOP	ns		****		****		****	

Polymer response greater

ns=no significant difference

* = $p<0.05$

*** = $p<0.005$

Polymer response less

** = $p<0.01$

**** = $p<0.0001$